ARTICLE

Ligand Size Effect on PdL_n Oxidative Addition with Aryl Bromide: A DFT Study

Wen-jing Sun[a], Wei Chu[a*], Liang-jun Yu[b], Cheng-fa Jiang[a*]

a. Department of Chemical Engineering, Sichuan University, Chengdu 610065, China
b. Hunan Zhongchuang Chemical Co. Ltd., Yueyang 414012, China

(Dated: Received on November 10, 2009; Accepted on February 18, 2010)

The process and mechanism of the ligand volume controlled $Pd(PR_3)_2$ (PR_3=PH_3, PMe_3, and $PtBu_3$) oxidative addition with aryl bromide were investigated, using density functional theory method with the conductor-like screening model. Association pathway and dissociation pathway were investigated by the comparison of several energies. The cleavage energy of $Pd(PR_3)_2$ complex was calculated, as well as the oxidative addition reaction barrier energy of $Pd(PR_3)_n$ (n=1, 2) with aryl bromide in N,N-dimethylformamide solvent. This study proved that the ligands volume possessed a great impact on the mechanism of oxidative addition: less bulky ligand palladium associated with aryl bromide via two donor ligands, but larger bulky ligand palladium coordinated via monoligand.

Key words: Process simulation, Ligand size effect, Oxidative addition, Cross-coupling reaction, DFT method

I. INTRODUCTION

Cross-coupling reactions were catalyzed by palladium species, were very useful in organic synthesis areas [1−4]. Unsaturated and highly donated ligands palladium complexes such as phosphine, were usually used to improve the catalytic activity in cross-coupling reactions [5−9]. A promising application is using them in the catalytic systems that can activate unreactive aryl halides, such as aryl bromides and chlorides, instead of iodobenzene as substrate, because those aryl halides are cheaper and more readily available to be compared with iodobenzene [10]. However, the challenge was that these halides were more reluctant to undergo catalytic reactions. Their C_{Ph}−X bonds are stronger which were more difficult to be broken in oxidative addition process [11, 12]. The oxidative addition process was the initial step and usually the rate limiting step in palladium-catalyzed cross-coupling reactions. In this process, aryl halide was added to PdL_n complex and generated a compound with σ-bound aryl groups (Fig.1). Galardon *et al.* studied series of complexes $[Pd(PC_ntBu_{3-n})]_2$, n=0−3 addition to ArI in tetrahydrafuran (THF) [13]. They found experimentally that the mechanism of the process was very sensitive to the volume of ligands. Their report explained and developed the disphosphine [14] and monophosphine pathways [15, 16]. Li *et al.* theoretically studied the monoligated Pd-catalyzed cross-coupling reactions of aryl chlorides and bromides [17]. They found that the oxidative addition mechanisms were very different with the different halide substrates and volume of ligand.

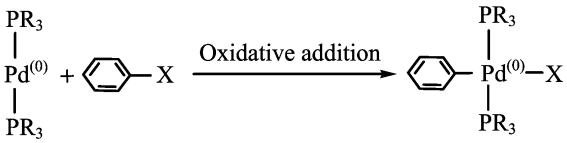

FIG. 1 Traditional oxidative addition.

In this work, the size effects of phosphine ligand were investigated in the reaction of oxidative addition PdL_n (n=1, 2) with aryl bromides. Three commonly used palladium phosphine complexes with different size (PR_3=PH_3, PMe_3, and $PtBu_3$) were used. We expected that the energy profiles of the reaction process would help to elucidate the relative importance of alternative pathways for the oxidative addition reaction.

II. CALCULATION METHODS

The calculations were performed with the dmol^3 [18, 19] program implemented within the Materials Studio of Accelrys, Inc. [20]. During the computation, exchange-correlation effects were described by the generalized approximation (GGA) [21] developed by Perdew, Burke and Ernzerhof (PBE) functional [22]. Using the double numerical polarized (DNP) basis sets for Pd, Br, and P, and double numerical basis set d-polarization function (DND) for C and H. The solvent phase was

*Author to whom correspondence should be addressed. E-mail: chuwei65@yahoo.com.cn, jiangcf1@yahoo.com, Tel.: +86-28-85403836, FAX: +86-28-85461108

TABLE I Optimized bond order and bond lengths in different phosphine ligands.

	Bond order	Bond length/Å
$Pd(PH_3)_2$	1.011	2.251
$PdPH_3$	1.468	2.148
$Pd(PMe_3)_2$	0.994	2.272
$PdPMe_3$	1.429	2.157
$Pd(PtBu_3)_2$	0.968	2.287
$PdPtBu_3$	1.383	2.172

represented by the COSMO (conductor-like screening model) [23] and the solvents parameters corresponding to N,N-dimethylformamide (DMF) (ε=36.7). Reaction energies were calculated:

$$\Delta E_{\text{reaction}} = E_{\text{products}} - E_{\text{reactants}} \quad (1)$$

$$E_{\text{barrier}} = E_{\text{TS}} - E_{\text{reaction}} \quad (2)$$

$E_{\text{reactants}}$, E_{TS}, and E_{products} were the energy of reactants, transition state complex, and products, respectively. Cleavage energy was calculated:

$$E = E_{\text{PdPR}_3)+E_{\text{PR}_3}-E_{\text{Pd(PR}_3)_2}} \quad (3)$$

optimized in DMF solvent.

The optimized geometries were also subjected to full frequency analysis at the same GGA/PBE level of theory to certify the nature of the stationary point. Transition state (TS) were performed at the same theoretical level with the complete linear synchronous transit (LST) and quadratic synchronous transition (QST) search methods (LST/QST) [24], then the transition state confirmation through the nudged elastic band (NEB) method [25].

III. RESULTS AND DISCUSSION

A. Optimized structures and parameters of $Pd(PR_3)_n$ (n=1, 2)

To identify the most likely starting point for the oxidative addition step, we calculated the properties of coordinative palladium phosphine species. Figure 2 shows the structures of three different diphosphine palladium complexes $Pd(PR_3)_2$ and their monophosphine palladium complexes $PdPR_3$ (PR_3=PH_3, PMe_3, and $PtBu_3$, respectively).

The $Pd(PR_3)_2$ complexes were summarily and linearly coordinated. Just as the structures reported by Lee [26], who optimized the structure of $Pd(PMe_3)_2$ with P−Pd−P bond angle of 180.0°. The correlative conformational parameters of these structures were shown in Table I and Table II. The Pd−P bond lengths were 2.251, 2.272, and 2.287 Å. Meanwhile, the bond orders were 1.011, 0.944, and 0.968 for PR_3=PH_3, PMe_3, and $PtBu_3$, respectively. Pd−P bond lengths elongated while the bond order decreased with the increasing size of ligand. The tendency reflected that bulky phosphine ligands might weaken the bond strength of Pd−P.

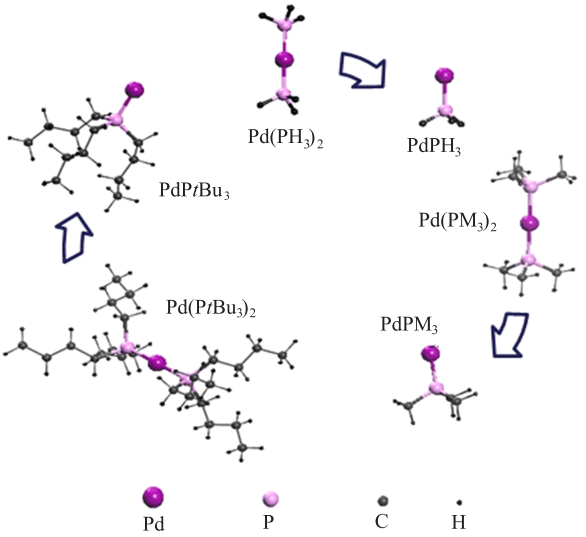

FIG. 2 Optimized structures for $Pd(PR_3)_2$ and $PdPR_3$. PR_3=PH_3, PMe_3, and $PtBu_3$.

After a phosphine dissociating from the diphosphine-palladium, the Pd−P bond lengths and bond order changed obviously. The Pd−P bond was shortened by 0.103, 0.115, and 0.115 Å for PR_3=PH_3, PMe_3 and $PtBu_3$, respectively. At the same time, the bond order was increased by 0.457, 0.435, and 0.415 accordingly, as a result of the strong *trans*-influence of phosphine. The same results were reported by Ahlquist *et al.* who found that the Pd−P bonds of $Pd(PPh_3)_2$ elongated by 0.1 Å compared to $PdPPh_3$ due to the *trans*-influence [27].

Cleavage energies of the $Pd(PR_3)_2$ was greatly related to bulkiness of the ligands. The cleavage energies were 62.127, 47.978, and 30.284 kJ/mol for PH_3, PMe_3, and $PtBu_3$, respectively. It seemed that the bulkier phosphine were easier to dissociate. Strieter *et al.* observed that less bulky phosphine of the palladium(II) complex resulted in slower dissociation in experiment. This indicated the importance of size of the supporting phosphine [28]. This may because of the stronger bond energy between Pd and P in less size of the supporting phosphine, such as $Pd(PH_3)_2$ and $Pd(Me_3)_2$.

B. Oxidative addition to $Pd(PR_3)_2$ (diphosphine pathway)

At the very beginning of oxidative addition, a tetracoordinated complex **1** was formed. Fan *et al.* confirmed that before the oxidative addition, a π-complex was formed by the palladium catalyst and the aryl halide [14]. In complex **1**, the P−Pd−P bond angle decreased to 111.35° in **1**H, 110.29° in **1**M from

DOI:10.1088/1674-0068/23/02/175-179

TABLE II The bond distances (in Å) and bond angles (in (°)) in reactants (**1** and **4**), the corresponding transition states (**2**-TS and **5**-TS) and products (**3** and **6**) of $Pd(PR_3)_n$ (n=1, 2) (PR_3=PH_3, PMe_3, $PtBu_3$) oxidative addition with bromobenzene.

	PH_3 (H)			PMe_3 (M)			$PtBu_3$ (B)		
	Pd−C_{ph}	Pd−Br	P1−Pd−P2	Pd−C_{ph}	Pd−Br	P−Pd−P			
1	2.206	3.338	111.35	2.151	3.414	110.29			
2-TS	2.093	2.716	106.28	2.104	2.784	112.27			
3	2.048	2.515	104.54	2.055	2.539	101.56			
	Pd−C_{ph}	Pd−P	P−Pd−Br	Pd−C_{ph}	Pd−P	P−Pd−Br	Pd−C_{ph}	Pd−P	P−Pd−Br
4	1.971	2.258	94.97	1.983	2.395	93.83	1.980	2.457	101.62
5-TS	1.970	2.468	136.05	1.964	2.472	130.76	2.034	2.459	138.50
6	1.982	2.429	175.00	1.984	2.260	170.89	1.978	2.269	166.93

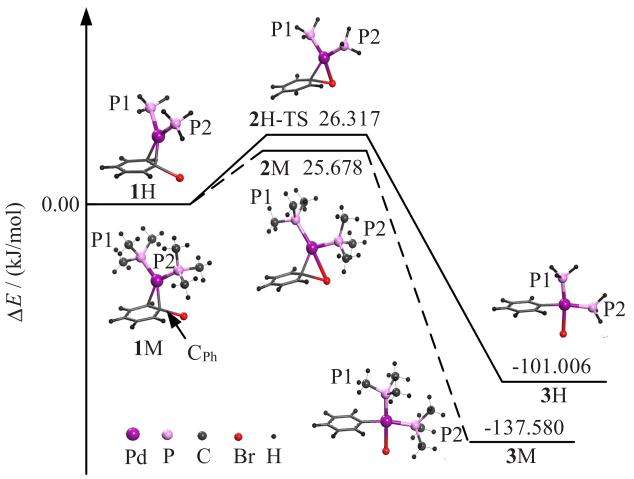

FIG. 3 Energy profile of $Pd(PR_3)_2$ oxidative addition to bromobenzene (PR_3=PH_3 (solid line) and PMe_3 (dashed line)). The energies were calculated in DMF solvent and given in kJ/mol.

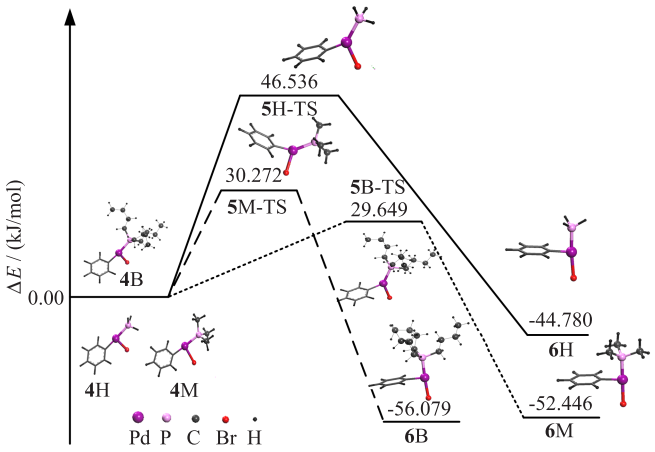

FIG. 4 Relative energy profile of $PdPR_3$ oxidation additive to bromobenzene (PR_3=PH_3 (solid line), PMe_3 (dotted line), and $PtBu_3$ (dashed line)). The energies were calculated in DMF solvent and given in kJ/mol.

nearly 180° in $Pd^{(0)}L_2$ complexes. Then the complex isomerizes through transition state **2**H-TS and **1**M-TS (Fig.3). In this process, Br anion migrated from bonding with C to bonding with Pd [25]. In the transition state structures, the Pd−Br distance was 2.716 Å in **2**H-TS, 2.784 Å in **2**M-TS, and the significant decreasing of Pd−Br distance can be found. Meanwhile, the P−Pd−P bond angle decreased to 106.28° in **2**H-TS and 112.27° in **2**M-TS with the accordingly barrier in oxidative addition of 26.317 and 25.678 kJ/mol for PR_3=PH_3 and PMe_3 in DMF solvent, respectively. Toro-Labbe and Rincon reported the process from reactant to transition state was structural rearranged and took place in the early stage of the reaction coordinate by the reaction force as a function [29]. The generation of products was exothermic process (ΔE=−101.006 and −137.580 kJ/mol for **3**H and **3**M, respectively). After that, the productions, a square-planar palladium complex **3**H and **3**M were formed. Due to the strong *trans* influence of phenyl ligand, the Pd−C_{Ph} bond was elongated by 0.1 Å comparing with **1**H and **1**M (2.206 and 2.151 Å, respectively). Pd−Br distance in **3**H and **3**M was 2.515 and 2.539 Å, respectively, which stood for the formation of the Pd−Br bonds.

However, the transition state of $Pd(PtBu_3)_2$ oxidative addition with ArBr could not be located. Hartwig and Paul detected the pathways of $Pd[P(o\text{-tolyl})_3]_2$ oxidative addition to aryl bromide by NMR spectrometer probe [8]. They found that the steric effects inhibited the oxidative addition reaction to occur through PdL_2 when L=P(o-tolyl)$_3$.

C. Oxidative addition with $PdPR_3$ (monophosphine pathway)

An alternative pathway was dissociation, by which the oxidative addition took place after losing a phosphine. The process of $PdPR_3$ oxidative addition to phenyl bromide was still a structural rearrangement process. The energy profile was shown in Fig.4. P−Pd−Br angles of the reactant (**4**H, **4**M, and **4**B)

DOI:10.1088/1674-0068/23/02/175-179

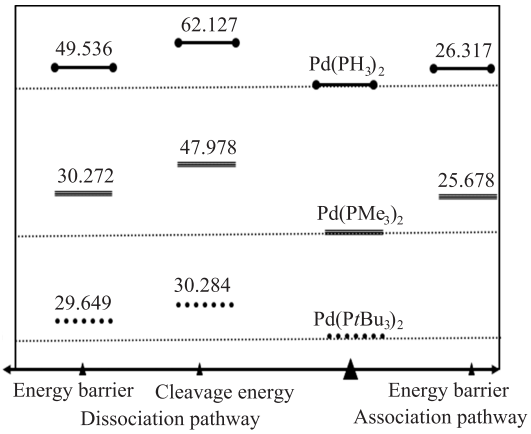

FIG. 5 Cleavage energy and the oxidative addition barrier energy of different diphosphine palladium and monophosphine palladium in DMF solvent in kJ/mol.

were 94.97°, 93.84°, and 101.62°, respectively. In the transition states (**5**H-TS, **5**M-TS, and **5**B-TS), the angle increased to 136.05°, 130.76°, and 138.50° respectively. The corresponding barrier of monophosphine oxidative addition was 46.536, 30.272, and 29.649 kJ/mol for PR_3=PH_3, PMe_3, and P*t*Bu_3, respectively. Compared to PMe_3 and P*t*Bu_3, it was more difficult for $PdPH_3$ to overcome the oxidative addition, due to weaker donating ability of PH_3 [5]. Following process was the transition state rearranged to a T-shaped structure **6**H, **6**M, and **6**B, the exothermic process gave the energy of 44.780, 52.446, and 56.079 kJ/mol.

Stambuli *et al.* provided extensive structural data of three-coordinate arylpalladium halide complexes by X-ray diffraction and computational studies [6, 7]. The X-ray crystal structures of $PdPhXPR_3$ showed that the structure had a T-shaped geometry with the phenyl ring locating *trans* to the open coordination site of the metal. The computational results of this work were consistent with the structure. The P−Pd−Br angles were 175.00°, 170.89°, and 166.93° for PR_3=PH_3, PMe_3, and P*t*Bu_3, respectively. And the bond length of Pd and C_{Ph} was approximately 1.98 Å for all the structures.

D. Comparison of different pathways

Based on the results previously discussed, an energy profile in different pathways could be drawn in Fig.5. Obviously, the cleavage energy of $Pd(PH_3)_2$ and that of $Pd(PMe_3)_2$ were higher than the energy barrier of they directly oxidative addition to bromobenzene (nearly 35.9 and 22.1 kJ/mol for PH_3 and PMe_3, respectively). Meanwhile, the $Pd(PH_3)_2$ energy barrier was nearly 25.1 kJ/mol, which was approximately to $Pd(PMe_3)_2$. Therefore, the $Pd(PH_3)_2$ and $Pd(Me_3)_2$ oxidative addition with bromobenzene was followed by an associative mechanism as shown in Fig.6.

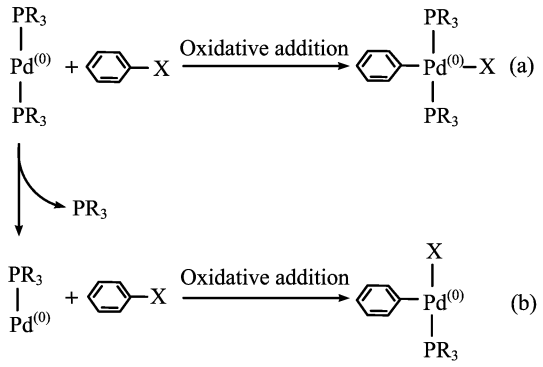

FIG. 6 Pathways of different size of ligand on the oxidative addition with bromobenzene. (a) For the less bulky phosphines, such as PH_3 and PMe_3. (b) For the large bulky phosphines, such as P*t*Bu_3.

On the other hand, the energy of dissociating a phosphine from $Pd(PtBu_3)_2$ was comparable to the barrier of monophsphine oxidative addition to bromobenzene, and the transition state of diphosphine could not be located. Therefore, the bulkier ligands favor dissociating before oxidative addition.

IV. CONCLUSION

In this study, density functional theory was used to study the ligand size effect on the $Pd(PR_3)_n$ (n=1, 2), PR_3=PH_3, PMe_3, and P*t*Bu_3 oxidative addition with aryl bromide. The cleavage energy of diphosphine palladium species and the barrier energy of bromobenzene oxidative addition with diphosphine palladium and monophosphine palladium were displayed. Meanwhile, the structures along the different reaction pathways were also located. The results revealed that the bulkier phosphine-palladium complexes undergone oxidative addition via monophosphine palladium, while the less bulky phosphine palladium complex undergone oxidative addition via diphosphine palladium.

V. ACKNOWLEDGMENTS

This work was supported by the National Natural Science Foundation of China (No.20776089) and the New Century Excellent Talents Program of Ministry of Education (No.NCET-05-0783). The State Key Laboratory of Polymer Materials Engineering in Sichuan University was acknowledged for providing dmol^3 modules and Prof. Ying Xue, Xiang-yuan Li, and Quan Zhu were grateful for the useful discussions.

[1] N. Miyaura and A. Suzuki, Chem. Rev. **95**, 2457 (1995).

DOI:10.1088/1674-0068/23/02/175-179

[2] A. D. Meijere and F. E. Meyer, Angew. Chem. Int. Ed. Engl. **33**, 2379 (1994).
[3] A. F. Littke and G. C. Fu, Angew Chem. Int. Ed. **41**, 4176 (2002).
[4] R. F. Heck, Org. React. **27**, 345 (1982).
[5] I. P. Beletskaya and A. V. Cheprakov, Chem. Rev. **100**, 3009 (2000).
[6] J. P. Stambuli, M. Buhl, and J. F. Hartwig, J. Am. Chem. Soc. **124**, 9346 (2002).
[7] J. P. Stambuli, C. D. Incarvito, M. Buehl, and J. F. Hartwig, J. Am. Chem. Soc. **126**, 1184 (2004).
[8] J. F. Hartwig and F. Paul, J. Am. Chem. Soc. **117**, 5373 (1995).
[9] L. J. Goossen, D. Koley, H. L. Hermann, and W. Thiel, Organometallics **24**, 2398 (2005).
[10] N. J. Whitcome, K. K. (Mimi) Hii, and S. E. Gibson, Tetrahedron **57**, 7449 (2001).
[11] W. A. Herrmann, C. Broßmer, K. Öfele, M. Beller, and H. Fischer, J. Mol. Catal. A: Chem. **103**, 133 (1995).
[12] R. Z. Zhang, X. H. Li, and X. Z. Zhang, Chin. J. Chem. Phys. **22**, 235 (2009).
[13] E. Galardon, S. Ramdeehul, J. M. Brown, A. Cowley, K. Hii, and A. Jutand, Angew. Chem. Int. Ed. **41**, 1760 (2002).
[14] W. Cabri and I. Candiani, Acc. Chem. Res. **28**, 2 (1995).
[15] P. Surawatanawong, Y. Fan, and M. B. Hall, J. Organomet. Chem. **693**, 1152 (2008).
[16] T. Yamamoto, M. Nishiyama, and Y. Koie, Tetrahedron Lett. **39**, 2367 (1998).
[17] Z. Li, Y. Fu, Q. X. Guo, and L. Liu, Organometallics **27**, 4043 (2008).
[18] J. P. Perdew and M. Levy, Phys. Rev. B **56**, 16021 (1997).
[19] X. Zhang, W. Chu, and J. J. Chen, Acta Phys. Chim. Sin. **23**, 45 (2009).
[20] B. Delley, J. Chem. Phys. **92**, 508 (1990).
[21] J. P. Perdew, J. A. Chevary, S. H. Vosko, K. A. Jackson, M. R. Pederson, D. J. Singh, and C. Fiolhais, Phys. Rev. B **46**, 6671 (1992).
[22] J. P. Perdew, K. Burke, and M. Ernzerhof, Phys. Rev. Lett. **77**, 3865 (1996).
[23] A. Klamt and G. Schüürmann, J. Chem. Soc. Perkin Trans. **2**, 799 (1993).
[24] B. Delley, J. Phys. Chem. **100**, 6107 (1996).
[25] G. Henkelman and H. Jónsson, J. Chem. Phys. **113**, 9978 (2000).
[26] M. T. Lee, M. H. Lee, and H. C. Hu, Organometallics **26**, 1317 (2007).
[27] M. Ahlquist, P. Fristrup, D. Tanner, and P. O. Norrby, Organometallics **25**, 2066 (2006).
[28] E. R. Strieter, D. G. Blackmond, and S. L. Buchwald, J. Am. Chem. Soc. **125**, 13978 (2003).
[29] E. Rincon and A. Toro-Labbe, Chem. Phys. Lett. **438**, 93 (2007).

DOI:10.1088/1674-0068/23/02/175-179